© 2019. Published by The Company of Biologists Ltd | Journal of Cell Science (2019) 132, jcs236505. doi:10.1242/jcs.236505

RESEARCH ARTICLE

Two conserved glycine residues in mammalian and *Dictyostelium* Rictor are required for mTORC2 activity and integrity

Barbara Pergolizzi[1], Cristina Panuzzo[1], M. Shahzad Ali[1], Marco Lo Iacono[1], Chiara Levra Levron[2], Luca Ponzone[2], Marta Prelli[2], Daniela Cilloni[1], Enzo Calautti[2], Salvatore Bozzaro[1] and Enrico Bracco[3,*]

ABSTRACT

Mammalian, or mechanistic, target of rapamycin complex 2 (mTORC2) regulates a variety of vital cellular processes, and its aberrant functioning is often associated with various diseases. Rictor is a peculiar and distinguishing mTORC2 component playing a pivotal role in controlling its assembly and activity. Among extant organisms, Rictor is conserved from unicellular eukaryotes to metazoans. We replaced two distinct, but conserved, glycine residues in both the *Dictyostelium piaA* gene and its human ortholog, *RICTOR*. The two conserved residues are spaced ∼50 amino acids apart, and both are embedded within a conserved region falling in between the Ras-GEFN2 and Rictor_V domains. The effects of point mutations on the mTORC2 activity and integrity were assessed by biochemical and functional assays. In both cases, these equivalent point mutations in the mammalian *RICTOR* and *Dictyostelium piaA* gene impaired mTORC2 activity and integrity. Our data indicate that the two glycine residues are essential for the maintenance of mTORC2 activity and integrity in organisms that appear to be distantly related, suggesting that they have a evolutionarily conserved role in the assembly and proper mTORC2 functioning.

KEY WORDS: Mammalian target of rapamycin, mTOR, AKT, PKB, *Dictyostelium*, Protein–protein interaction, Rictor

INTRODUCTION

Mammalian, or mechanistic, target of rapamycin (mTOR) is a serine/threonine kinase that belongs to the phosphatidylinositol 3-kinase-related kinase (PIKK) family. mTOR forms two functionally distinct multi-protein complexes, namely mTOR complex 1 (mTORC1) and mTOR complex 2 (mTORC2), which differ in the regulatory subunits with which they associate (Zoncu et al., 2011). For instance, regulatory associated protein of TOR (Raptor) and proline-rich Akt substrate of 40-kDa (PRAS40) (also known as RPTOR and AKT1S1, respectively, in mammals) are mTORC1-specific constituents, whereas rapamycin-insensitive companion of TOR (Rictor), Stress-activated map kinase-interacting protein 1 (Sin1; also known as MAPKAP1) and protein observed with Rictor 1 and 2 (Protor1/2; also known as PRR5 and PRR5L, respectively), are specific for mTORC2. Other proteins, like the TOR kinase itself, LST8 (also known as GβL and MLST8) and DEP domain-containing TOR-interacting protein (Deptor) are shared instead between mTORC1 and mTORC2.

With few notable exceptions, restricted to plants and some Alveolata species, both TOR complexes are conserved among extant organisms ranging from unicellular eukaryotes to animals (Tatebe and Shiozaki, 2017). Both mTOR complexes (mTORCs) function as multimers by sensing environmental cues and/or stress conditions, thus ensuring a correct integration of the intracellular and extracellular signals to promote cell growth, survival, metabolism and motility (Sarbassov et al., 2005). Dysregulation of mTOR signaling is observed in virtually all solid tumours and hematologic malignancies, as well as in several neurodegenerative and metabolic disorders (Dinner and Platanias, 2016; Lan et al., 2017; Linke et al., 2017; Pópulo et al., 2012). While mTORC1 acts predominantly on eukaryotic translation initiation factor 4E-binding protein (14E-BP1) and p70/S6 kinase (p70/S6K) substrates, mTORC2 phosphorylates AGC kinases such as AKT1 (also known as protein kinase B, PKB; hereafter denoted AKT), serum and glucocorticoid-activated kinase (SGK) and protein kinase C (PKC) family members, thereby regulating their activation and/or protein stability (Guertin et al., 2006). Currently available mTOR inhibitors show promiscuous activity towards mTORC1 and mTORC2, although rapamycin derivatives (Rapalogs) are rather selective for mTORC1 during a short incubation (Kim et al., 2002). The availability of small molecules capable of selective mTORC2 inhibition still remains an unmet need.

Essential for the design of specific mTORC2 inhibitors is the detailed resolution of its 3D structure, as well as the elucidation of the molecular mechanisms underlying both its proper regulation as well its malfunctioning, which presently are still poorly understood.

Hitherto, the use of simple and genetically amenable model organisms has been extremely beneficial for the investigation of mTORC2 regulation. *Dictyostelium discoideum* is a social amoeba that has long been used as a model system for studying fundamental processes in cell and development biology (Bozzaro, 2013). *Dictyostelium* cells grow and divide mitotically but, upon starvation, undergo a developmental program in which cells form multicellular aggregates through chemotaxis, and eventually fruiting bodies (Bozzaro, 2013). Unlike yeast, but similar to what is found in animals, the *Dictyostelium discoideum* genome encodes for a single TOR kinase, and mTORC2 is a key player in many cellular processes. Single and multiple mutants in the diverse mTORC2 components have been generated and phenotypically characterized (Lee et al., 2005). As in other organisms, targeted gene disruption of the *Dictyostelium rictor* ortholog (*piaA*) gene (Chen et al., 1997), henceforth referred to as *pia*, led to severe developmental defects, mostly due to the inability to activate downstream G-protein coupled receptor (GPCR) signaling pathways, such as those mediated by adenylyl cyclase A (ACA) and AKT (Kamimura et al., 2010). Among

[1]Department of Clinical and Biological Sciences, University of Torino, AOU S. Luigi, 10043 Orbassano (TO), Italy. [2]Department of Molecular Biotechnology and Health Sciences, Molecular Biotechnology Centre, University of Torino, Via Nizza 52, 10126 Torino, Italy. [3]Department of Oncology, University of Torino, AOU S. Luigi, 10043 Orbassano (TO), Italy.

*Author for correspondence (enrico.bracco@unito.it)

E.B., 0000-0003-3170-2817

Received 15 July 2019; Accepted 15 October 2019

Journal of Cell Science (2019) 132, jcs236505. doi:10.1242/jcs.236505

Dictyostelium mTORC2 mutants, we isolated and characterized a temperature-sensitive aggregation-deficient strain, named HSB1 (Bozzaro et al., 1987). HSB1 harbors a point mutation at codon 917 in the *pia* gene, resulting in the amino acid change G917D (Pia^{G917D}). At the non-permissive temperature, HSB1 cells phenocopied *pia*-null cells (Pergolizzi et al., 2002). Besides the Pia mutation affecting the mTORC2 activity, a missense mutation (G1120E) of the *C. elegans rictor* gene (*rict-1*) has been isolated and characterized. The corresponding mutation in mammals (Rictor^{G934E}) was shown to prevent Rictor binding to Sin1 and consequently the assembly of a functional mTORC2 (Aimbetov et al., 2012).

Although Rictor family members do not possess clearly identifiable structural protein domains or motifs, they share regions of different length that are classified by PFAM and SMART prediction software as Rictor_N, Rictor_M, Ras-GEFN2, Rictor_V and Rictor Phospho (Sarbassov et al., 2004). The structural and functional properties of these conserved regions is still unknown.

In the present study, we carried out a comparative analysis of the biochemical and cellular phenotypes of two distinct Pia and Rictor mutants (Jones et al., 2009; Pergolizzi et al., 2002; Soukas et al., 2009), both altered in two conserved glycine residues, in cells of the social amoeba *D. discoideum* and *Homo sapiens*. We show that, despite the evolutionary distance between these organisms, both mutations cause similar biochemical and cellular effects.

RESULTS

Architectural domain evolution of Rictor proteins and localization of functional glycine residues

Rictor is the largest mTORC2 protein subunit, and performs key scaffolding function that are likely analogous to that of Raptor in stabilizing the dimerization of mTORC1 (Sarbassov et al., 2004). A detailed phylogenetic analysis revealed that, although Rictor members are present in many phyla, their architectural organization is significantly different among various species (Fig. S1). Evolutionary analysis, based on the presence or absence of different motifs as predicted by PFAM and SMART algorithms, highlighted that even among the same clade, Rictor proteins showed significant architectural variance. Indeed, among animals, when comparing Chordata with Platyhelminthes and with Echinodermata, we noticed that Rictor family members were poorly structurally characterized. By contrast some lower eukaryotes (e.g. yeast and amoebas) displayed a Rictor architecture closer to that of Chordata than to other animal species (e.g. Echinodermata and Platyhelminthes).

The detailed examination of the single point mutations that are so far known to impair mTORC2 activity (Pia^{G917D} and *H. sapiens* Rictor^{G934E}), revealed that both of these glycine residues are embedded within a linker peptide spanning from the end of the Ras-GEFN2 until to the beginning of the Rictor_V domain, and in both cases a non-polar amino acid is replaced by a negatively polar charged residue. Remarkably, this region is predicted to be either disordered or show low complexity in a number of Rictor proteins. It is noteworthy that the mutated amino acid residues in the *D. discoideum* Pia^{G917D}, *C. elegans* Rictor^{G1068E} (formerly annotated as Rictor^{G1120E}; Jones et al., 2009) and *H. sapiens* Rictor^{G934E} are rather well conserved among different phyla and are located within the second and the third repeated block of ∼30 amino acids, that represent a shared feature of Rictor proteins (Sarbassov et al., 2004) (Fig. 1A).

Interestingly, within the region spanning between the Ras-GEFN2 and Rictor_V domains there are several conserved amino acids showing a very high level of identity that can peak as high as ∼70% (e.g. glycine residue corresponding to the position 892 in human Rictor) (Fig. 1B,C).

Although Rictor is an essential mTORC2 component, these analyses suggest that the global domain architecture differs significantly among various members. Therefore, establishing an accurate structure-to-function relationship appears rather challenging. By contrast, investigation of allelic variants affecting mTORC2 activity might represent a more-powerful tool to identify region(s) needed for mTORC2 integrity and function.

Dictyostelium Pia^{G963E} does not rescue the HSB1 phenotype and impairs the development of wild-type cells in a similar manner to Pia^{G917D}

The *Dictyostelium* temperature-sensitive strain HSB1, isolated as aggregation-deficient mutant, harbors a point mutation in the *pia* gene resulting in a single amino acid replacement at codon 917 (G917D) in the Pia protein. This mutation is responsible for the aggregation-deficient phenotype, resulting from the inability to activate ACA and thus to produce cyclic AMP (Pergolizzi et al., 2002). Cyclic AMP is essential in *Dictyostelium* development, because it acts as chemoattractant, hormone-like signal and intracellular second messenger, hence regulating both chemotaxis and the expression of genes required for aggregation and post-aggregative development (Du et al., 2015; Loomis, 2014; Pergolizzi et al., 2017a, 2002).

When reproducing the *H. sapiens* mutation (Rictor^{G934E}) in *Dictyostelium* cells (Pia^{G963E}), we observed that this mutation failed to rescue the HSB1 aggregation-deficient phenotype (Fig. 2A). Consistent with this, when expressed in AX2 cells, Pia^{G963E} resulted in delayed aggregation and fruiting body formation, as occurred with Pia^{G917D} (Pergolizzi et al., 2002) (Fig. 2B). However, the Pia^{G963E} protein was always found to be expressed at a lower level than the wild-type (wt) or G917 proteins, probably as result of a reduced protein stability, as was previously described for the corresponding Rictor^{G934E} human mutation (Aimbetov et al., 2012). Because this decreased protein stability is likely an intrinsic feature of both the *Dictyostelium* and the corresponding human mutation, we cannot formally rule out that the severe aggregation phenotype seen with this mutant may depend in part on its reduced protein level, besides an impaired TORC2 signaling activity. Considering that in parental AX2 cells the wt Pia is normally expressed, the aggregation and development delay observed when the mutated forms are overexpressed could be the result of competition for binding partners between the endogenous wt and the overexpressed mutated Pia proteins (Pergolizzi et al., 2002).

A high-resolution version of the 3D Rictor structure is presently missing, but these results indicate that the Pia mutant proteins impair mTORC2 activity, suggesting a key functional role for both of the conserved glycine residues located between the Ras-GEFN2 and Rictor_V domains.

Both Pia G917 and G963 are needed to preserve *Dictyostelium* mTORC2 integrity

We have previously shown that HSB1 cells fail to activate mTORC2 by assessing the phosphorylation status of the hydrophobic motif (HM) and activation loop (AL) of PKBA and PKBR1 as well as their phosphorylated substrates by means of phospho-specific antibodies (Pergolizzi et al., 2017b). Nevertheless, the question of whether the mutated Pia^{G917D} controlled mTORC2 integrity, or solely its kinase activity, remained unanswered. To address this issue, we examined the Pia–LST8 interaction in HSB1 cells

Journal of Cell Science (2019) 132, jcs236505. doi:10.1242/jcs.236505

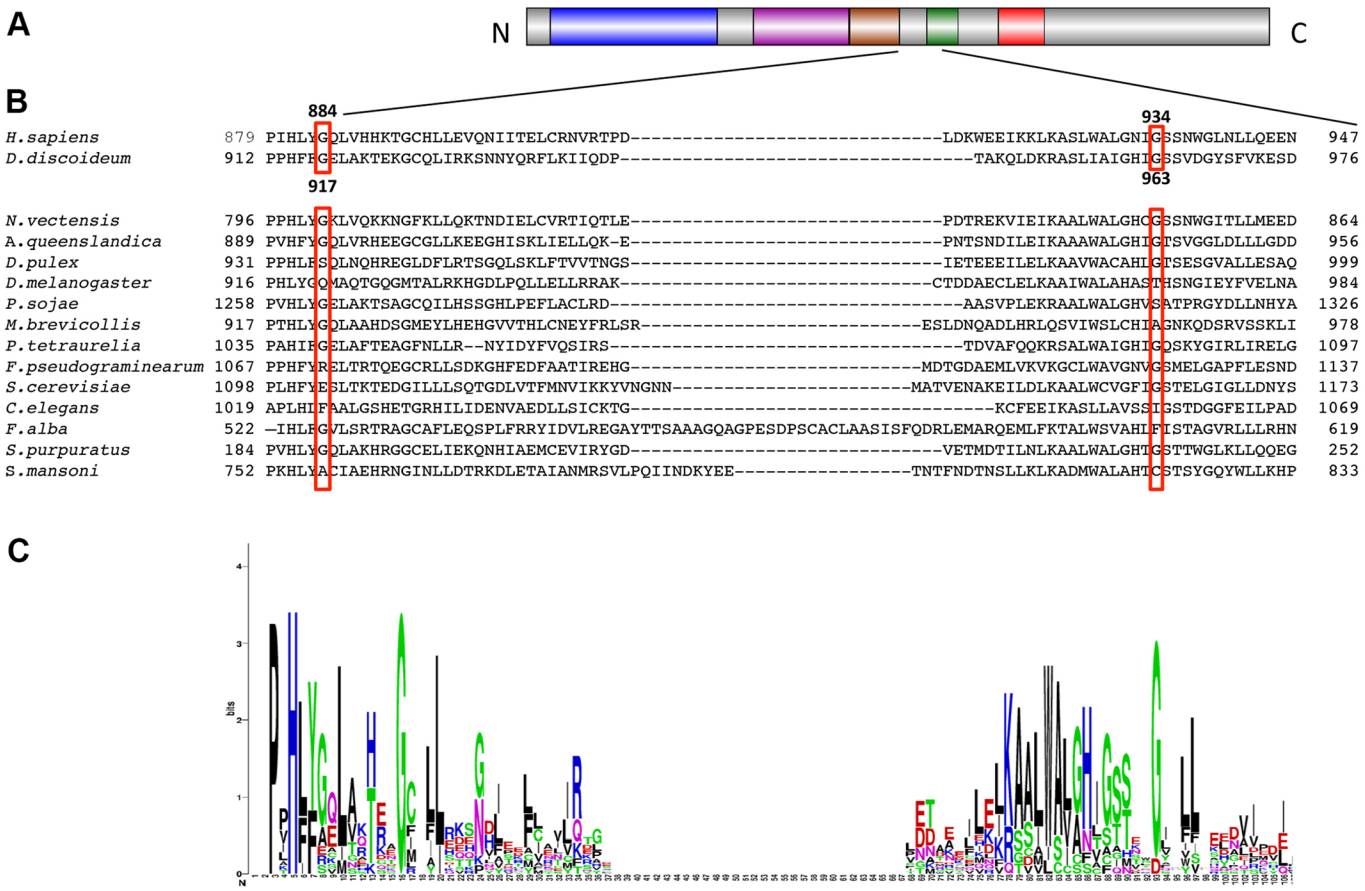

Fig. 1. Rictor protein architectural organization of the conserved regions and region encompassing the two conserved Gly residues. (A) Schematic representation of the mammalian Rictor protein conserved regions. Highly conserved regions of Rictor protein are shown in colored boxes: Rictor_N (blue), Rictor_M (purple), Ras-GEFN2 (yellow), Rictor_V (green) and Rictor_Phosho (red). (B) Multiple sequence alignment of the peptide region between Ras-GEFN2 and Rictor_V of different species: *Homo sapiens* (UniProt Q6R327); *Dictyostelium discoideum* (UniProt O77203); *Nematostella vectensis* (UniProt A7SRE9); *Amphimedon queenslandica* (UniProt A0A1X7UI29); *Daphnia pulex* (UniProt E9HCD6); *Drosophila melanogaster* (UniProt X2JL73); *Phytophthora sojae* (UniProt G4YPP8); *Monosiga brevicollis* (UniProt A9V5T2); *Paramecium tetraurelia* (UniProt A0EHS6); *Fusarium pseudograminearum* (UniProt K3VWR9); *Saccharomyces cerevisiae* (UniProt P40061); *Caenorhabditis elegans* (UniProt G5EFN2); *Fonticula alba* (UniProt A0A058ZD18); *Strongylocentrotus purpuratus* (UniProt W4Y7H9); and *Schistosoma mansoni* (UniProt G4VPY8). The *Dictyostelium* G917 site aligns with the human G884, whereas the human G934 aligns with the *Dictyostelium* G963 residue. The red rectangles in the multiple sequence alignment indicate the conserved residues among different clades. Protein sequences alignment was performed with MUSCLE (www.ebi.ac.uk/Tools/nsa/muscle/). (C) WebLogo depicting the multiple sequence alignment of the peptide sequence spanning between Ras-GEFN2 and Rictor_V of the different Rictor proteins. The logo consists of stacks of letters with one stack for each position in the sequence. The overall height of the stacks indicates the relative frequency of each amino acid at that position. The logo was generated by using WebLogo (http://weblogo.berkeley.edu/logo.cgi), a web-based application designed to generate sequence logos.

stably co-expressing Pia^{wt}, Pia^{G917D} or Pia^{G963E}, and LST8. The interaction between LST8 and mutated Pia proteins was severely impaired when compared to Pia^{wt} (Fig. 3). This means that like *Dictyostelium* Pia G917, Pia G963 is also an additional residue required for the proper assembly of TORC2, in agreement with the previously reported observations in mammalian cells (Aimbetov et al., 2012).

Considering the high degree of conservation in the connecting Ras-GEFN2-to-Rictor_V peptide among different Rictor family members (Fig. 1) and the biological/biochemical effects caused by both mutations on mTORC2 integrity, we surmise that both of these two glycine residues may be essential for the proper integrity and/or signaling activity of *Dictyostelium* TORC2.

Mammalian Rictor G884 is required for mTORC2 full activity and partially controls its integrity

Since when reproduced in *Dictyostelium*, the human Rictor^{G934E} mutation affects TORC2 activity by interfering with the integrity of the complex, as occurs in mammals, we also decided to investigate the effects of the corresponding *Dictyostelium* mutation Pia^{G917D} in the context of the human Rictor protein (Rictor^{G884D}).

Hence, we took advantage of a recently developed Rictor-knockout (KO) A375 melanoma cell line developed in our laboratory via CRISPR/Cas9 technology. As shown in Fig. 4A, these cells do not display any detectable Rictor expression as compared to wt A375 cells. While in wt A375 cells, phosphorylation of bona fide mTORC2 protein targets, such as AKT (at S473) was increased upon serum stimulation, in the Rictor KO counterparts its level was nearly abolished even in presence of serum. Moreover in the knockout cells, phosphorylation of PKCα at S657, another known mTORC2 target site, was drastically diminished along with the total levels of AKT and PKCα proteins, consistent with the notion that mTORC2 also regulates the overall stability of these proteins. In contrast, phosphorylation of the mTORC1 substrate 4EBP1 at T37 and T46 (T36/47) was similar to that of wt cells. Altogether, these findings indicate that this A375

Journal of Cell Science (2019) 132, jcs236505. doi:10.1242/jcs.236505

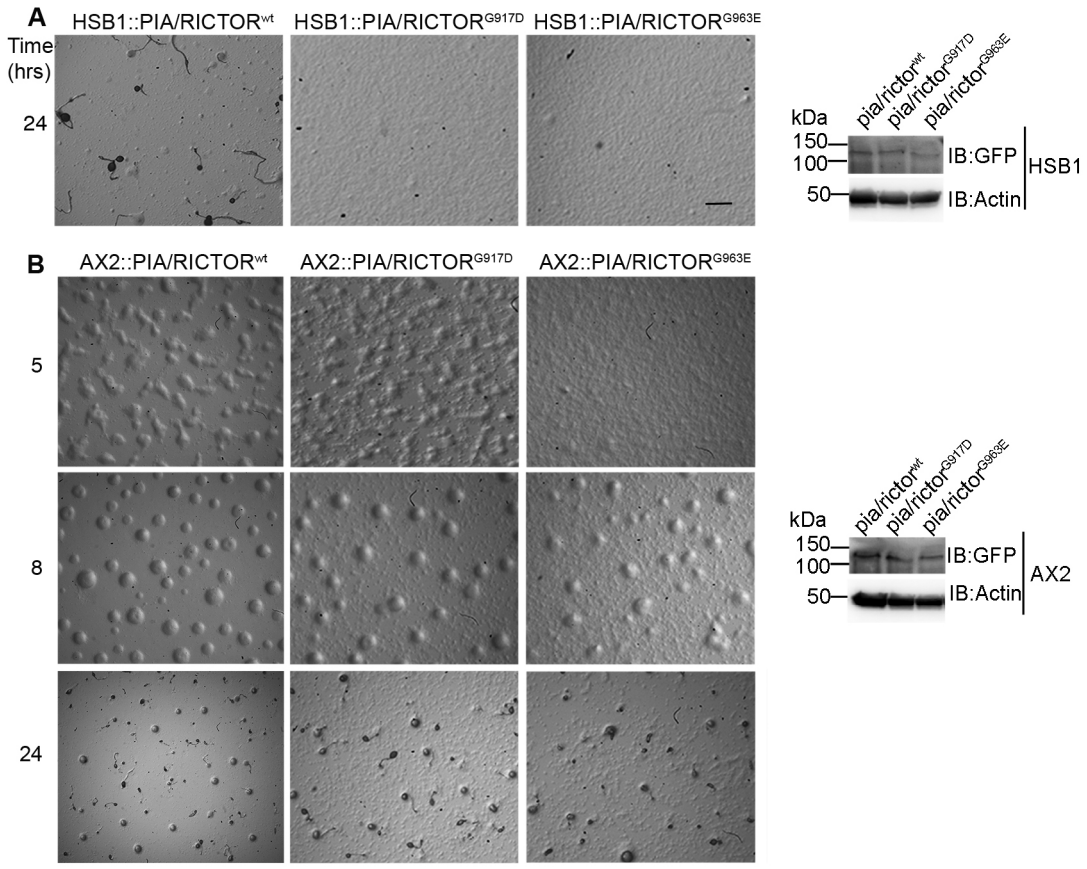

Fig. 2. Phenotype of HSB1 and AX2 *Dictyostelium* cells overexpressing wt *pia* and its mutated forms. HSB1 (A) and AX2 (B) cells were transfected with *pia*^{wt} (*pia*/*rictor*^{wt}), *pia*^{G917D} (*pia*/*rictor*^{G917D}) or *pia*^{G963E} (*pia*/*rictor*^{G963E}) genes (tagged with GFP). A 0.03 ml drop, at a concentration of 10^7/ml of the selected clones, was plated on non-nutrient agar and development followed for 24 h. Experiments were carried-out at a temperature of 23°C. AX2::Pia/Rictor^{G917D} and AX2::Pia/Rictor^{G963E} display a delay in the onset of aggregation and development. Several single cells are visible after 24 h of development. HSB1::Pia/Rictor^{G917D} and HSB1:: Pia/Rictor^{G963E} fail to aggregate in contrast to HSB1::Pia/Rictor^{wt} where fruiting bodies are detectable. Photographs were taken at the indicated times. The immunoblots (IB) beside each set revealed the relative amount of the Pia protein expressed for each strain. Scale bar: 0.5 mm.

Rictor KO cell line faithfully recapitulates features typical of selective mTORC2 disruption in different cellular models (Guertin et al., 2006; Tassone et al., 2017).

It has been previously reported that the low proliferation rate observed in mammalian cells expressing the mutated Rictor^{G934E} is due to inactive mTORC2 because of its inability to assemble a mature complex (Aimbetov et al., 2012); therefore, we first determined the effects of Rictor^{G884D} on cell proliferation. Rictor KO cells were transiently transfected with either human Rictor^{wt} or with the mutated forms (Rictor^{G884D} or Rictor^{G934E}) and cell proliferation was assessed using cells transfected with empty vector as baseline control.

As shown in Fig. 4B, whereas expression of human Rictor^{wt} led to increased proliferation when compared to the control, neither of the Rictor mutants had a significant effect on cell proliferation, as revealed by an MTT assay.

We next examined the phosphorylation status of AKT S473, a canonical mTORC2 substrate. The phosphorylation levels of AKT at this site were lower in the Rictor KO A375 cells expressing Rictor^{G884D}, Rictor^{G934E} or the empty vector, as compared to the control cells expressing Rictor^{wt}. Moreover, in cells expressing mutant Rictor proteins, the phosphorylation profiles evidenced by an antibody detecting the 'canonical' phosphorylated motif typical of AKT- and other AGC-directed kinase substrates differed from those of cells expressing wt Rictor, suggesting alterations in downstream signaling (Fig. 5A). Cells expressing the mutant Rictor^{G934E}, as detected by phosphorylation on S473, showed severe impairment in kinase activity as previously reported (Aimbetov et al., 2012).

Since the Pia^{G917D} mutation interferes with *Dictyostelium* mTORC2 integrity, we decided to examine whether Rictor^{G884D} could also interfere with the mammalian mTORC2 assembly by assessing the Rictor^{G884D}–Sin1 and Rictor^{G884D}–LST8 interactions in HEK 293T cells. Notably, in contrast to what occurs for Rictor and Sin1, the interaction between Rictor and LST8 is not the result of their direct association. Nevertheless, LST8 is an essential mTORC2 component that is required to regulate its kinase activity (Guertin et al., 2006; Lee et al., 2005).

The human Rictor^{G884D} mutation did not significantly interfere with the interaction of the protein with Sin1 (~30% less compared to the wt form), which is different from what was been previously observed with the Rictor^{G934E}, for which this interaction is severely compromised (Fig. S2). Despite the fact that Rictor^{G934E} protein levels in A375 cells were lower than those of Rictor^{G884D} and Rictor^{wt}, the effects on the mTORC2 signaling outputs are likely more severe than those caused simply by its reduced expression (~80% inhibition of AKT phosphorylation when normalized for Rictor revels; see Fig. 5B), although we cannot formally rule out that also reduced protein dosage also contributes to the inability of the mutant to support cellular growth, as shown in Fig. 4B.

Journal of Cell Science (2019) 132, jcs236505. doi:10.1242/jcs.236505

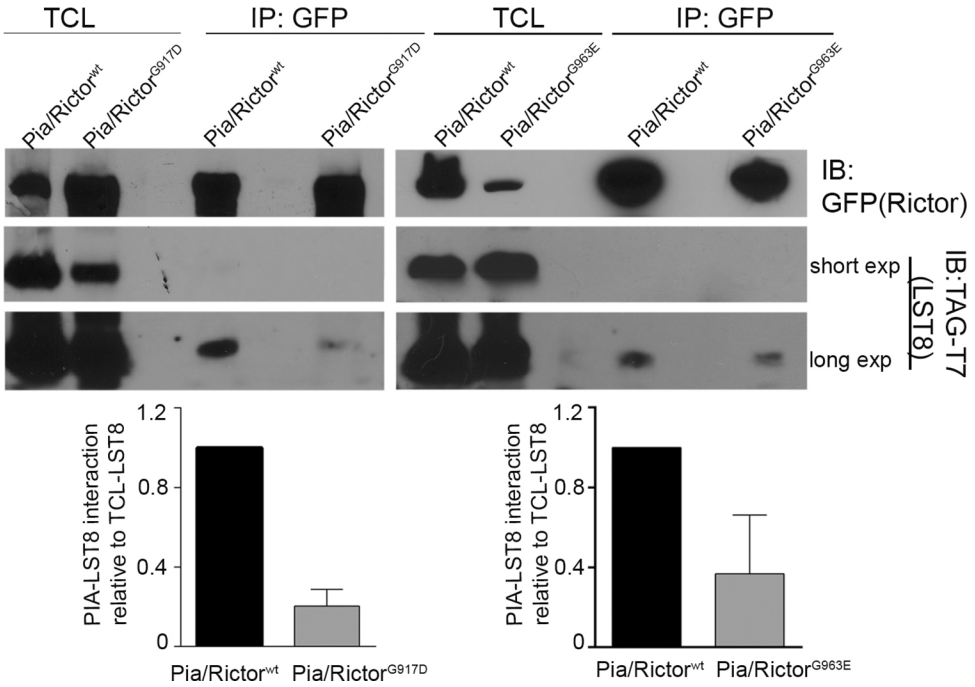

Fig. 3. Pia G917 and G963 are both necessary for the mTORC2 integrity. wt or mutated GFP-tagged *pia* plasmids [*pia*^{wt} (*pia*/*rictor*^{wt}), *pia*^{G917D} (*pia*/*rictor*^{G917D}) or *pia*^{G963E} (*pia*/*rictor*^{G963E})] were co-expressed together with the LST8-T7 plasmid in AX2 cells. Cells starved for 4 h were then lysed at 4°C and the soluble fraction isolated by centrifugation. For immunoprecipitation (IP), GFP-trap beads were added to the cleared cellular lysates followed by overnight incubation with rotation at 4°C. Immunoprecipitates were analyzed for the indicated proteins by immunoblotting. The mutated forms of Pia display a very low binding to LST8 in comparison with the wt. The lower expression level detected in the total cell lysate (TCL) for Pia/Rictor^{G963E} when compared to the wt form might be due to a weaker protein stability, as occurs for the mammalian counterpart Rictor^{G934E} (Aimbetov et al., 2012). The bands intensities, corresponding to LST8 protein, were quantified using ImageJ. For every experimental condition (Pia/Rictor^{wt} against the two mutated Pia forms) the highest amount of LST8 measured in TCL samples was given the value of 1. Afterwards, the TCL LST8 ratio calculated between the Pia^{wt} and the mutated Pia forms was used to normalize the corresponding LST8 co- immunoprecipitated bands. To optimize signals, shorter and longer exposures of a representative experiment are shown. The normalized mean±s.d. of at least three different experiments are plotted in the bar graphs.

By contrast, the Rictor^{G884D}–LST8 interaction is impaired to a higher extent than the Rictor^{G884D}–Sin1 interaction (Fig. 5B). In summary, these results indicate that the *Dictyostelium* mutation, when reproduced in mammalian cells, not only impairs mTORC2 kinase activity but also partially interferes with the complex integrity by reducing the incorporation of LST8 within TORC2.

DISCUSSION

Since the identification of mTORC2 as the main kinase responsible for phosphorylation of the AKT S473, necessary for its maximal activation, there has been an increasing body of evidence indicating that mTORC2/AKT signaling dysregulations are associated with the initiation and progression of several cancer types, as well as in the

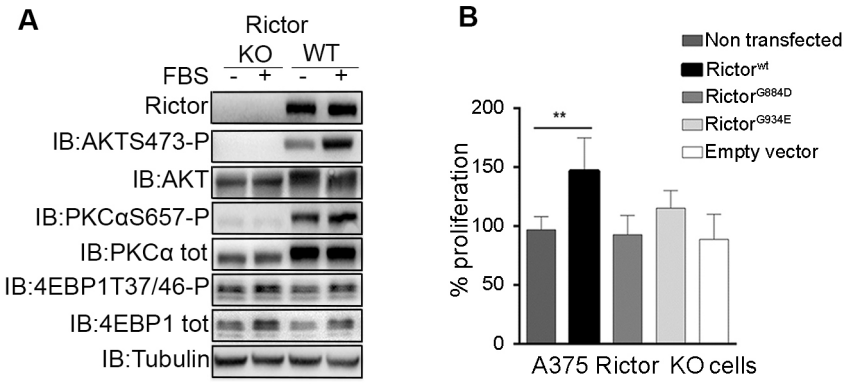

Fig. 4. Biochemical and functional characterization of A375 Rictor KO cells. (A) Normal (wt) or Rictor knockout (KO) A375 cells were starved for 24 h and then treated (+) or not (–) with FBS for 15 min. Afterwards, total cell lysates (TCLs) were analyzed by immunoblotting with the indicated antibodies detecting phosphorylated and total mTORC2 and mTORC1 target proteins. (B) Rictor mutated forms affect cell proliferation. A proliferation assay was performed in A375 cells knocked out for Rictor and transfected with the indicated Rictor mutants or empty vector. The assay was performed 48 h after transfection by seeding 10,000 cells per well in triplicates for each condition. The bar graph represents mean±s.d. values expressed as a percentage for at least three different experiments relative to the proliferation obtained with Rictor KO A375 (set at 100%). Only transfection of wt human Rictor resulted in an increased proliferation rate when compared to the control Rictor KO cells. ***P*<0.01 (Student's *t*-test).

Journal of Cell Science (2019) 132, jcs236505. doi:10.1242/jcs.236505

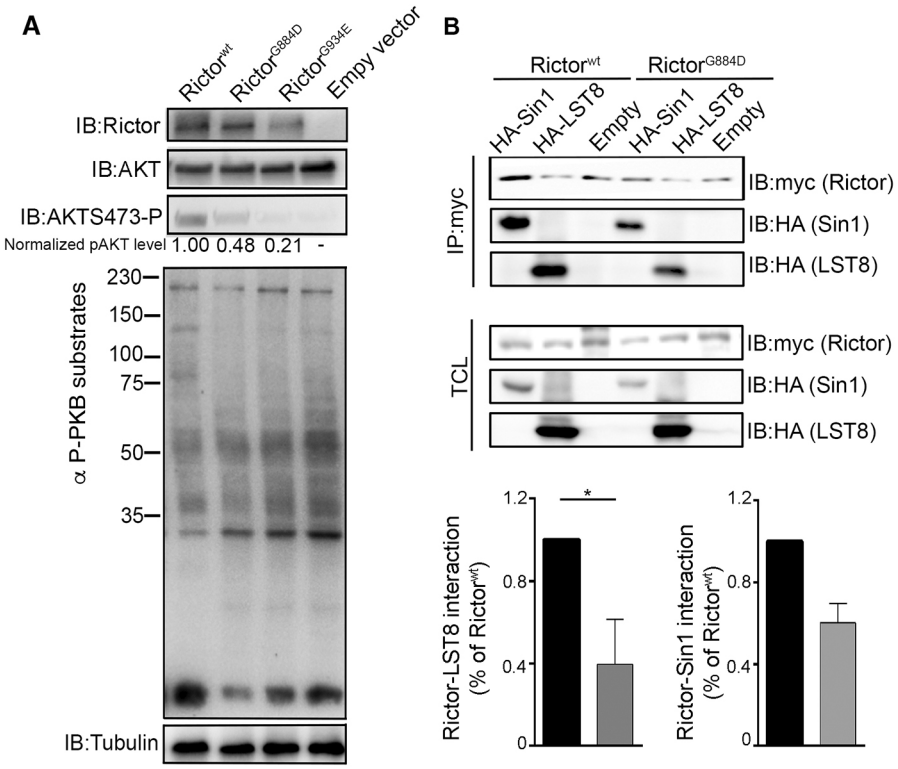

Fig. 5. Rictor mutations interfere with mTORC2 activity and integrity. (A) Rictor mutant forms impair mTORC2 activity. Immunoblot (IB) analysis of mTORC2 substrate phospho-AKT S473 (pAKT, AKTS473-P) and AKT substrates (α-P-PKB substrates) in A375 Rictor KO cells transfected with Rictor^{wt} or mutants. AKT phosphorylation is significantly reduced in the Rictor KO A375 cells expressing Rictor^{G884D}, Rictor^{G934E} or empty vector, when compared to the control cells expressing the wt form of Rictor. Values underneath the corresponding lanes represent the normalized levels of p-AKT adjusted for the corresponding Rictor protein levels. The wt level was set at 1. The signal from empty vector-transfected cells (background level) was subtracted from other values. Data represent the mean of two independent experiments. (B) Rictor^{G884D} interferes with mTORC2 integrity. Immunoprecipitation of Rictor in HEK 293T cells co-transfected with either Rictor^{wt} or Rictor^{G884D} together with Sin1 or LST8. For immunoprecipitation (IP) Myc-trap beads were used. After 1 h of incubation, immunocomplexes were washed and subsequently analyzed by western blotting. Quantification of Sin1 and LST8 immunoprecipitated with Rictor were normalized to the Sin1 and LST8 values obtained with the Rictor^{wt} form. Bar graphs represent the mean±s.d. of three independent experiments. *P<0.05 (Student's t-test).

pathogenesis of neurodegenerative and metabolic disorders (e.g. diabetes) (Johnson et al., 2015; Pópulo et al., 2012). Therefore, there is a growing interest in selectively targeting the mTORC2/AKT signaling axis. Rictor, together with Sin1, is an essential mTORC2 component critical for its assembly. Alterations of Rictor itself have also been identified in several cancer types including prostate cancer, lung squamous cell carcinoma, sarcoma and stomach cancer (Cheng et al., 2015; Kim et al., 2017). However, since its identification, the structural and functional properties of the unique conserved regions of the Rictor protein have remained rather elusive.

With the present comparative study, for the first time, we have elucidated the functions of two Pia point mutations in regulating mTORC2 activity and integrity in a robust evolutionary conserved manner. The mutations we analyzed are localized both within an ∼60-amino-acid long peptide that is embedded between the conserved Ras-GEFN2 and Rictor_V regions. Remarkably, these mutations affect residues that are conserved between the lower eukaryote *Dictyostelium* and the human Rictor. Our results show that, in *Dictyostelium* cells, the Pia^{G917D} mutation impairs the mTORC2 activity because it interferes with the integrity of the complex. When we reproduced the same mutation in the human Rictor (G884D), the resulting protein altered the mTORC2 kinase activity and integrity, although to a lesser extent than the corresponding *Dictyostelium* mutation Pia^{G917D}. The partial inconsistency between *Dictyostelium* Pia^{G917D} and mammalian Rictor^{G884D} could be due to several reasons. The *Dictyostelium* HSB1 strain, harboring the Pia^{G917D}, has been isolated as temperature-sensitive strain indicating that the effect caused by the mutation might be by-passed by shifting the cells to a lower temperature. Indeed, HSB1 cells fail to aggregate at 23°C, but aggregate and develop normally at temperatures below 18°C (Pergolizzi et al., 2002). In many Rictor proteins from different species, the linker peptide connecting the Ras-GEFN2 and Rictor_V is characterized by an apparently low complexity or disordered structure that conceivably is more prone to conformational transitions upon temperature or energy changes. Moreover, although both mammals and *Dictyostelium* share the same mTORC2 components, they slightly differ in their structural composition. Several Rictor proteins from different organisms, as well as the *Dictyostelium* Pia, structurally diverge from that of Chordata due to their smaller size and because they lack the so-called Rictor-Phospho region.

Currently, it is plausible to hypothesize that the weaker Rictor^{G884D}–LST8 interaction, observed in human cells, is responsible for the impaired kinase activity, given that LST8 is crucial for the enzymatic regulation of mTORC2 (Guertin et al., 2006). The *Dictyostelium* Sin1 ortholog (Rip3) does not possess a PH domain, leaving unanswered the question of how *Dictyostelium* mTORC2 is recruited to the plasma membrane. In addition, mTORC2 components might act in a TOR-independent way (Gao et al., 2010; Hagan et al., 2008; McDonald et al., 2008; Zhang et al., 2010). Consistent with this, in *Dictyostelium* the *Rip3*-null and *Pia*-null phenotypes differ substantially, suggesting that the role of these proteins is not strictly and exclusively restricted to mTORC2 (Lee et al., 2005). Overall, these differences may explain the slightly distinct biochemical behavior that we have observed between *Dictyostelium* and mammalian cells.

The second mutation analyzed in *Dictyostelium* cells corresponded to human Rictor^{G934E}, which was already known to interfere with the human mTORC2 activity and integrity (Aimbetov et al., 2012). The same mutation in *Dictyostelium* Pia did not rescue the aggregation-deficient HSB1 phenotype and delayed aggregation in wt AX2 cells, similar to what was seen for the endogenous G917D mutation. These data strongly indicate that mTORC2 remained inactive. Consistent with this, the biochemical characterization confirmed that mTORC2 failed to assemble into a mature complex, as occurred for the Pia^{G917D} mutation, strengthening the hypothesis that in *Dictyostelium*, similar to in mammalian cells, adenylyl cyclase

Journal of Cell Science (2019) 132, jcs236505. doi:10.1242/jcs.236505

activation requires mTORC2 (Liu et al., 2010). The effects of the Pia^{G963E} mutation are considerably detrimental despite the lower protein amount when compared to the wt counterpart. Overall, these data suggest that Pia^{G963E}, when expressed in wt strain cells, avidly competes with the endogenous wt protein, thus acting as dominant negative. Additionally, these observations lead us to presume that, in Pia, the replacement of a non-polar glycine residue with a negatively charged one, such as glutamate (E) at codon 963, likely enhances the protein instability. Given that a similar behavior has also been observed for human Rictor, it is reasonable to assume that the glycine residue is evolutionarily important from amoebas to human, because it affects the protein stability. Further experiments will be required to elucidate the reason(s) leading to weaker Pia^{G963E} and Rictor^{G934E} stability.

The finding that the functional characterization of these two mutations in different cell types leads to similar results indicates that these glycine residues play a crucial, and evolutionary conserved, role either in regulating mTORC2 kinase activity or, to different extent, integrity. Remarkably, none of these mutations is annotated as a single nucleotide polymorphism (SNP) and both are predicted to be hazardous/deleterious by PolyPhen-2 (Adzhubei et al., 2010) and SIFT/PROVEAN (Kumar et al., 2009). A missense point mutation affecting the human *RICTOR* gene at codon 855 (R855W), closely located to the amino acids we analyzed, has been predicted to be deleterious and associated with Tourette syndrome (Eriguchi et al., 2017). These findings, together with our results, suggest that the peptide spanning from Ras-GEFN2 to Rictor_V represents a crucial regulator for mTORC2.

How these glycine residues are mechanistically essential for regulating mTORC2 enzymatic activity and integrity still remains elusive. The recently reported *S. cerevisiae* TORC2 structure reveals a rhombohedral pseudo-two-fold symmetric shape with a pronounced central cavity resembling that of mTORC1. Nevertheless, the exact surfaces mediating the assembly, substrate specificity and enzymatic activity, as well as the role of the prominent central cavity, remain rather enigmatic and not entirely identified (Karuppasamy et al., 2017). Intra- and inter-molecular crosslinking data suggest that Avo3, the yeast ortholog of the mammalian Rictor, wraps around TOR2 and that parts of AVO3 are very close to the FKBP12 rapamycin-binding domain (FRB). The AVO3 amino acid residues corresponding to those we have investigated in the present study might be localized very near to the FRB, thus likely assigning this region a crucial role in regulating the kinase activity. A computational investigation, using combined bioinformatic tools, has examined the sequence and structural properties of the human Rictor protein, revealing that Rictor possesses a HEAT and WD40 domain, further identifying a ribosome-binding domain and two possible PH domains, one of which splits (Zhou et al., 2015). Interestingly, the mutations we have analyzed are localized around the predicted PH domains. Based on the current and previous findings, we assume that whereas the G934 is essential for the Rictor–Sin1 heterodimer formation, the G884 residue is needed for the correct assembly of the LST8 into mTORC2. Although LST8 is not a unique mTORC2 component, it is essential for the kinase activity thus its partial displacement leads to impaired enzymatic activity. Overall, these data suggest that these residues are crucial for the regulation of the TOR complex 2 by controlling the supramolecular protomer assembly.

Despite the recent advances in exploring the 3D structure of mTORC2, our understanding of its regulation and signaling outputs is still rudimentary, thus the issue of whether potential mTORC2-specific inhibitors will be clinically useful remains hypothetical. Within this scenario, our present findings reveal that mutations in two conserved glycine residues in Rictor, initially found in mammals and *Dictyostelium*, exhibit common effects when present in either organism, indicating that these residues play a pivotal role in regulating mTORC2 activity and integrity. Furthermore, we provided evidence that *Dictyostelium* might represent a novel and useful model tool to improve our current knowledge concerning mTORC2 enzymatic regulation. Gaining molecular insights into mTORC2 assembly and regulation, by making use of simple model organisms, would facilitate the rational design of compounds that (i) prevent or disrupt mTORC2 assembly, (ii) block access of substrates to the active site, (ii) prevent the interaction of upstream activators, or (iv), in some cases, hyper-activate mTORC2.

MATERIALS AND METHODS

Dictyostelium discoideum cell culture and development

Parental AX2 and mutant HSB1 strains were cultured axenically in AX2 medium (Ashworth and Watts, 1970) at 23°C under shaking at 150 rpm as previously described (Pergolizzi et al., 2017b). For inducing development, exponentially growing cells were washed twice in 0.017 M Soerensen Na/K phosphate buffer, pH 6.1, resuspended at 10^7 cells per ml and starved for the indicated time either plated on non-nutrient agar or incubated under shaking at 150 rpm, as previously described (Pergolizzi et al., 2017b).

Dictyostelium plasmids construction and generation of cell lines co-expressing wt or mutated Pia with LST8

GFP–*pia* expression vectors were constructed as previously described (Pergolizzi et al., 2002). The *piaA*^{wt} gene was used as template to generate the mutated *pia*^{G963E} form using the QuikChange II site-directed mutagenesis kit (Agilent Technologies, catalog # 200518) with specific primers named FORWPia^{G963E} and REVPia^{G963E} (Table S1).

The G963E mutation was verified by DNA sequencing. The plasmids obtained were used to transfect AX2 and HSB1 cells to generate stable cell lines. Positive clones were selected for their resistance to G418 (20 µg/ml) and visually screened by fluorescence microscopy (Peracino et al., 2006).

The wt or mutated GFP-tagged Rictor plasmids were co-electroporated with the LST8 overexpressor plus T7-tag vector (plasmid #247, http://dictybase.org) in AX2 cells. G418-resistant clones were isolated and subjected to western blotting to identify those expressing both proteins.

Mammalian cell culture

A375 melanoma (ATCC CRL-1619) and human embryonic kidney 293T (provided by Guido Serini, Dept. of Oncology, University of Torino, Italy) cell lines were maintained in DMEM supplemented with 10% fetal bovine serum (FBS), 500 U/ml penicillin and 0.5 mg/ml streptomycin as previously described (Panuzzo et al., 2015). Cells were cultured at 37°C in a humidified atmosphere flushed with 5% CO_2.

CRISPR/Cas9-induced A375 Rictor KO melanoma cell lines were generated as follows. First, two independent sgRNAs targeted to human *RICTOR* exon 3 were selected using the UCSC Genome Browser [target sequences: 5′-CCATCTGAATAACTTTACTA-3′ (Sg1) and 5′-CCTTAGTAAAGTTATTCAGA-3′ (Sg2)]. Double-stranded DNA oligonucleotides encoding for Sg1 and Sg2 were cloned into the BsbI site of the pSpCas9 (BB)-2A-Puro (PX459) V2.0 plasmid (Addgene #62988; Ran et al., 2013). Subconfluent A375 cells were transfected with 4 µg of Sg1- or Sg2-carrying plasmid using Lipofectamine® 2000 in six-well plates. After 24 h, cells were then selected with puromycin (2 µg/ml) for a further 48 h. After selection, individual colonies were isolated with cloning disks and analyzed for Rictor protein expression and phosphorylation or expression of bona fide mTORC2 target proteins. Rictor KO clones generated with Sg1 were used in the present study.

When needed, serum stimulation was performed as follows: cells were serum starved for 24 h and then stimulated for 15 min with 10% FBS.

Homo sapiens plasmid construction and transient protein expression

myc-RICTOR (plasmid #11367), HA-SIN1 (plasmid #12583) and HA-LST8 (plasmid #1865) (Sarbassov et al., 2004) were purchased from Addgene. The Rictor plasmids harboring G884E and G934E mutations, were generated using the QuikChange II site-directed mutagenesis kit (Agilent Technologies, catalog #200518). For the mutagenesis reaction, we employed the Rictor^{wt} plasmid as template and the primers FORWRictor^{G934E}H.s., REVRictor^{G8934E}H.s., FORWRictor^{G884D}H.s. and REVRictor^{G884D}H.s. (Table S1). For transient transfection, the plasmids were transfected either in A375 or HEK 293T cells using Lipofectamine® (Lipofectamine 2000, Thermo Fisher Scientific) according to the manufacturer's instruction.

Proliferation assay

Mammalian cell proliferation was assessed via an MTT assay (Sigma-Aldrich) as described previously (Di Savino et al., 2015). Briefly, cells were plated in 96-well plates by seeding 10,000 cells per well and grown for 48 h. Afterwards, MTT was added and samples incubated at 37°C for approximately a couple of hours and absorbance measured at OD 590 nm using a plate reader. The obtained staining was proportional to the number of proliferating cells. The data are expressed as a percentage with respect to the not transfected cells, set to 100%, as the mean values±standard deviation (s.d.) of at least three independent experiments. Each condition was performed in a technical triplicate.

Cell lysis, immunoprecipitation and western blotting

Dictyostelium and mammalian total protein cell extraction was performed as described previously (Aimbetov et al., 2012). Protein extracts were further clarified by centrifugation at 12,000 ***g*** for 15 min at 4°C and subsequently quantified with a Bradford protein assay (BioRad Laboratories, CA). For immunoprecipitation, ∼1.5 mg of total protein extracts were processed with Myc-TRAP or GFP-TRAP beads (Myc-TrapA and GFP-TrapA, Chromotek, Germany).

Afterwards, samples were resolved by SDS-PAGE (8% gels) and subsequently transferred onto PVDF membrane. Immunoblots were then probed overnight at 4°C with specific antibodies in TBS (NaCl 150 mM, Tris-HCl 20 mM pH7.4), 0.1% Tween, 1% BSA, and protein detection performed by using peroxidase-conjugated secondary antibodies and chemiluminescence reagent (Clarity Western ECL Substrate #170-5061, Bio-Rad). Primary antibodies against the following were used: AKT (#9272 Cell Signaling Technology, 1:1000); phospho-AKT S473 (sc-7985-R Santa Cruz Biotechnology, 1:1000); phospho-Akt Substrate (RXXS*/T*) (#9614 Cell Signaling Technology, 1:1000), phospho-PKCα Ser-657 (#06-822, UpState, 1:1000), PKCα (sc-208 Santa Cruz Biotechnology, 1:1000), Rictor (sc-271081, Santa Cruz Biotechnology, 1:250), T7 TAG (A190-217A Bethyl, 1:1000), GFP, from *Dictyostelium* community (Westphal et al., 1997), Myc (#2276 Cell Signaling Technology, 1:1000), phospho-4E-BP1 Thr37/46 (#2855 Cell Signaling Technology, 1:1000), 4E-BP1 (#9452 Cell Signaling Technology, 1:1000) and tubulin (#T5168, Sigma-Aldrich, 1:1000). Films were exposed for different time periods to optimized signals.

Acknowledgements

We are thankful to Prof. Emilia Turco and Dr Fiorella Balzac for help with the CRISPR/Cas9 technology and to Prof. Guido Serini for providing HEK 293T cells.

Competing interests

The authors declare no competing or financial interests.

Author contributions

Conceptualization: B.P., S.B., E.B.; Methodology: B.P., C.P., M.S.A., M.L.I., C.L.L., L.P., M.P., E.B.; Validation: B.P., C.P., M.S.A., C.L.L., L.P., M.P., D.C., E.C., E.B.; Investigation: B.P., C.P., M.L.I., E.B.; Data curation: B.P., C.P., M.S.A., M.L.I., C.L.L., L.P., M.P., E.C., E.B.; Writing - original draft: B.P., E.B.; Writing - review & editing: B.P., E.C., S.B., E.B.; Visualization: B.P., D.C., E.C., E.B.; Supervision: B.P., E.C., S.B., E.B.; Project administration: B.P., E.B.; Funding acquisition: B.P., D.C., E.C., S.B.

Funding

This research was supported by a Compagnia di San Paolo grant (12-CSP-C03-065) to S.B., research funding from the Università degli Studi di Torino to B.P., Ministero dell'Istruzione, dell'Università e della Ricerca (PRIN 2015) to E.C. and Associazione Italiana per la Ricerca sul Cancro (5x1000) to D.C.

Supplementary information

Supplementary information available online at
http://jcs.biologists.org/lookup/doi/10.1242/jcs.236505.supplemental

References

Adzhubei, I. A., Schmidt, S., Peshkin, L., Ramensky, V. E., Gerasimova, A., Bork, P., Kondrashov, A. S. and Sunyaev, S. R. (2010). A method and server for predicting damaging missense mutations. *Nat. Methods* **7**, 248-249. doi:10.1038/nmeth0410-248

Aimbetov, R., Chen, C.-H., Bulgakova, O., Abetov, D., Bissenbaev, A. K., Bersimbaev, R. I. and Sarbassov, D. D. (2012). Integrity of mTORC2 is dependent on the rictor Gly-934 site. *Oncogene* **31**, 2115-2120. doi:10.1038/onc.2011.404

Ashworth, J. M. and Watts, D. J. (1970). Metabolism of the cellular slime mould Dictyostelium discoideum grown in axenic culture. *Biochem. J.* **119**, 175-182. doi:10.1042/bj1190175

Bozzaro, S. (2013). The model organism Dictyostelium discoideum. *Methods Mol. Biol.* **983**, 17-37. doi:10.1007/978-1-62703-302-2_2

Bozzaro, S., Hagmann, J., Noegel, A., Westphal, M., Calautti, E. and Bogliolo, E. (1987). Cell differentiation in the absence of intracellular and extracellular cyclic AMP pulses in Dictyostelium discoideum. *Dev. Biol.* **123**, 540-548. doi:10.1016/0012-1606(87)90412-X

Chen, M.-Y., Long, Y. and Devreotes, P. N. (1997). A novel cytosolic regulator, Pianissimo, is required for chemoattractant receptor and G protein-mediated activation of the 12 transmembrane domain adenylyl cyclase in Dictyostelium. *Genes Dev.* **11**, 3218-3231. doi:10.1101/gad.11.23.3218

Cheng, H., Zou, Y., Ross, J. S., Wang, K., Liu, X., Halmos, B., Ali, S. M., Liu, H., Verma, A., Montagna, C. et al. (2015). Rictor amplification defines a novel subset of patients with lung cancer who may benefit from treatment with mtorc1/2 inhibitors. *Cancer Discov.* **5**, 1262-1270. doi:10.1158/2159-8290.CD-14-0971

Di Savino, A., Panuzzo, C., Rocca, S., Familiari, U., Piazza, R., Crivellaro, S., Carrà, G., Ferretti, R., Fusella, F., Giugliano, E. et al. (2015). Morgana acts as an oncosuppressor in chronic myeloid leukemia. *Blood* **14**, 2245-2253. doi:10.1182/blood-2014-05-575001

Dinner, S. and Platanias, L. C. (2016). Targeting the mTOR pathway in leukemia. *J. Cell. Biochem.* **117**, 1745-1717. doi:10.1002/jcb.25559

Du, Q., Kawabe, Y., Schilde, C., Chen, Z.-H. and Schaap, P. (2015). The evolution of aggregative multicellularity and cell-cell communication in the Dictyostelia. *J. Mol. Biol.* **427**, 3722-3733. doi:10.1016/j.jmb.2015.08.008

Eriguchi, Y., Kuwabara, H., Inai, A., Kawakubo, Y., Nishimura, F., Kakiuchi, C., Tochigi, M., Ohashi, J., Aoki, N., Kato, K. et al. (2017). Identification of candidate genes involved in the etiology of sporadic Tourette syndrome by exome sequencing. *Am. J. Med. Genet. B Neuropsychiatr. Genet.* **174**, 712-723. doi:10.1002/ajmg.b.32559

Gao, D., Wan, L., Inuzuka, H., Berg, A. H., Tseng, A., Zhai, B., Shaik, S., Bennett, E., Tron, A. E., Gasser, J. A. et al. (2010). Rictor forms a complex with Cullin-1 to promote SGK1 ubiquitination and destruction. *Mol. Cell* **39**, 797-808. doi:10.1016/j.molcel.2010.08.016

Guertin, D. A., Stevens, D. M., Thoreen, C. C., Burds, A. A., Kalaany, N. Y., Moffat, J., Brown, M., Fitzgerald, K. J. and Sabatini, D. M. (2006). Ablation in mice of the mTORC components raptor, rictor, or mLST8 reveals that mTORC2 is required for signaling to Akt-FOXO and PKCalpha, but not S6K1. *Dev. Cell* **11**, 859-871. doi:10.1016/j.devcel.2006.10.007

Hagan, G. N., Lin, Y., Magnuson, M. A., Avruch, J. and Czech, M. P. (2008). A Rictor-Myo1c complex participates in dynamic cortical actin events in 3T3-L1 adipocytes. *Mol. Cell. Biol.* **28**, 4215-4226. doi:10.1128/MCB.00867-07

Johnson, J. L., Huang, W., Roman, G. and Costa-Mattioli, M. (2015). TORC2: a novel target for treating age-associated memory impairment. *Sci. Rep.* **5**, 15193. doi:10.1038/srep15193

Jones, K. T., Greer, E. R., Pearce, D. and Ashrafi, K. (2009). Rictor/TORC2 regulates Caenorhabditis elegans fat storage, body size, and development through sgk-1. *PLoS Biol.* **7**, e60. doi:10.1371/journal.pbio.1000060

Kamimura, Y., Cai, H. and Devreotes, P. (2010). 6-TORC2 and chemotaxis in Dictyostelium discoideum. *Enzymes* **28**, 125-142. doi:10.1016/S1874-6047(10)28006-X

Karuppasamy, M., Kusmider, B., Oliveira, T. M., Gaubitz, C., Prouteau, M., Loewith, R. and Schaffitzel, C. (2017). Cryo-EM structure of Saccharomyces cerevisiae target of rapamycin complex 2. *Nat. Commun.* **8**, 1729. doi:10.1038/s41467-017-01862-0

Kim, D.-H., Sarbassov, D. D., Ali, S. M., King, J. E., Latek, R. R., Erdjument-Bromage, H., Tempst, P. and Sabatini, D. M. (2002). mTOR interacts with raptor

to form a nutrient-sensitive complex that signals to the cell growth machinery. *Cell* **110**, 163-175. doi:10.1016/S0092-8674(02)00808-5

Kim, S. T., Kim, S. Y., Klempner, S. J., Yoon, J., Kim, N., Ahn, S., Bang, H., Kim, K.-M., Park, W., Park, S. H. et al. (2017). Rapamycin-insensitive companion of mTOR (RICTOR) amplification defines a subset of advanced gastric cancer and is sensitive to AZD2014-mediated mTORC1/2 inhibition. *Ann. Oncol.* **28**, 547-554. doi: 10.1093/annonc/mdw669

Kumar, P., Henikoff, S. and Ng, P. C. (2009). Predicting the effects of coding non-synonymous variants on protein function using the SIFT algorithm. *Nat. Protoc.* **4**, 1073-1081. doi:10.1038/nprot.2009.86

Lan, A.-P., Chen, J., Zhao, Y., Chai, Z. and Hu, Y. (2017). mTOR signaling in parkinson's disease. *Neuromolecular Med.* **19**, 1-10. doi:10.1007/s12017-016-8417-7

Lee, S., Comer, F. I., Sasaki, A., McLeod, I. X., Duong, Y., Okumura, K., Yates, J. R., Parent, C. A. and Firtel, R. A. (2005). TOR complex 2 integrates cell movement during chemotaxis and signal relay in Dictyostelium. *Mol. Biol. Cell* **16**, 4572-4583. doi:10.1091/mbc.e05-04-0342

Linke, M., Fritsch, S. D., Sukhbaatar, N., Hengstschläger, M. and Weichhart, T. (2017). mTORC1 and mTORC2 as regulators of cell metabolism in immunity. *FEBS Lett.* **591**, 3089-3103. doi:10.1002/1873-3468.12711

Liu, I., Das, S., Losert, W. and Parent, C. (2010). mTORC2 regulates neutrophil chemotaxis in a cAMP- and RhoA-dependent fashion. *Dev. Cell* **19**, 845-857. doi:10.1016/j.devcel.2010.11.004

Loomis, W. F. (2014). Cell signaling during development of Dictyostelium. *Dev. Biol.* **391**, 1-16. doi:10.1016/j.ydbio.2014.04.001

McDonald, P. C., Oloumi, A., Mills, J., Dobreva, I., Maidan, M., Gray, V., Wederell, E. D., Bally, M. B., Foster, L. J. and Dedhar, S. (2008). Rictor and integrin-linked kinase interact and regulate Akt phosphorylation and cancer cell survival. *Cancer Res.* **15**, 1618-1624. doi:10.1158/0008-5472.CAN-07-5869

Panuzzo, C., Volpe, G., Cibrario Rocchietti, E., Casnici, C., Crotta, K., Crivellaro, S., Carrà, G., Lorenzatti, R., Peracino, B., Torti, D. et al. (2015). New alternative splicing BCR/ABL-OOF shows an oncogenic role by lack of inhibition of BCR GTPase activity and an increased of persistence of Rac activation in chronic myeloid leukemia. *Oncoscience* **2**, 880-891. doi:10.18632/oncoscience.260

Peracino, B., Wagner, C., Balest, A., Balbo, A., Pergolizzi, B., Noegel, A. A., Steinert, M. and Bozzaro, S. (2006). Function and mechanism of action of Dictyostelium Nramp1 (Slc11a1) in bacterial infection. *Traffic* **7**, 22-38. doi:10.1111/j.1600-0854.2005.00356.x

Pergolizzi, B., Peracino, B., Silverman, J., Ceccarelli, A., Noegel, A., Devreotes, P. and Bozzaro, S. (2002). Temperature-sensitive inhibition of development in Dictyostelium due to a point mutation in the piaA gene. *Dev. Biol.* **251**, 18-26. doi:10.1006/dbio.2002.0809

Pergolizzi, B., Bozzaro, S. and Bracco, E. (2017a). G-Protein dependent signal transduction and ubiquitination in Dictyostelium. *Int. J. Mol. Sci.* **18**, E2180. doi:10.3390/ijms18102180

Pergolizzi, B., Bracco, E. and Bozzaro, S. (2017b). A new HECT ubiquitin ligase regulating chemotaxis and development in Dictyostelium discoideum. *J. Cell Sci.* **130**, 551-562. doi:10.1242/jcs.194225

Pópulo, H., Lopes, J. M. and Soares, P. (2012). The mTOR signalling pathway in human cancer. *Int. J. Mol. Sci.* **13**, 1886-1918. doi:10.3390/ijms13021886

Ran, F. A., Hsu, P. D., Wright, J., Agarwala, V., Scott, D. A. and Zhang, F. (2013). Genome engineering using the CRISPR-Cas9 system. *Nat. Protoc.* **8**, 2281-2308. doi:10.1038/nprot.2013.143

Sarbassov, D. D., Ali, S. M., Kim, D.-H., Guertin, D. A., Latek, R. R., Erdjument-Bromage, H., Tempst, P. and Sabatini, D. M. (2004). Rictor, a novel binding partner of mTOR, defines a rapamycin-insensitive and raptor-independent pathway that regulates the cytoskeleton. *Curr. Biol.* **14**, 1296-1302. doi:10.1016/j.cub.2004.06.054

Sarbassov, D. D., Ali, S. M. and Sabatini, D. M. (2005). Growing roles for the mTOR pathway. *Curr. Opin. Cell Biol.* **17**, 596-603. doi:10.1016/j.ceb.2005.09.009

Soukas, A. A., Kane, E. A., Carr, C. E., Melo, J. A. and Ruvkun, G. (2009). Rictor/TORC2 regulates fat metabolism, feeding, growth, and life span in Caenorhabditis elegans. *Genes Dev.* **23**, 496-511. doi:10.1101/gad.1775409

Tassone, B., Saoncella, S., Neri, F., Ala, U., Brusa, D., Magnuson, M. A., Provero, P., Oliviero, S., Riganti, C. and Calautti, E. (2017). Rictor/mTORC2 deficiency enhances keratinocyte stress tolerance via mitohormesis. *Cell Death Differ.* **24**, 731-746. doi:10.1038/cdd.2017.8

Tatebe, H. and Shiozaki, K. (2017). Evolutionary conservation of the components in the TOR signaling pathways. *Biomolecules* **7**, E77. doi:10.3390/biom7040077

Westphal, M., Jungbluth, A., Heidecker, M., Mühlbauer, B., Heizer, C., Schwartz, J.-M., Marriott, G. and Gerisch, G. (1997). Microfilament dynamics during cell movement and chemotaxis monitored using a GFP-actin fusion protein. *Curr. Biol.* **7**, 176-183. doi:10.1016/S0960-9822(97)70088-5

Zhang, F., Zhang, X., Li, M., Chen, P., Zhang, B., Guo, H., Cao, W., Wei, X., Cao, X., Hao, X. et al. (2010). mTOR complex component Rictor interacts with PKCzeta and regulates cancer cell metastasis. *Cancer Res.* **70**, 9360-9370. doi:10.1158/0008-5472.CAN-10-0207

Zhou, P., Zhang, N., Nussinov, R. and Ma, B. (2015). Defining the domain arrangement of the mammalian target of Rapamycin complex component Rictor protein. *J. Comput. Biol.* **22**, 876-886. doi:10.1089/cmb.2015.0103

Zoncu, R., Efeyan, A. and Sabatini, D. M. (2011). mTOR: from growth signal integration to cancer, diabetes and ageing. *Nat. Rev. Mol. Cell Biol.* **12**, 21-35. doi:10.1038/nrm3025

Supplementary data

Fig. S1

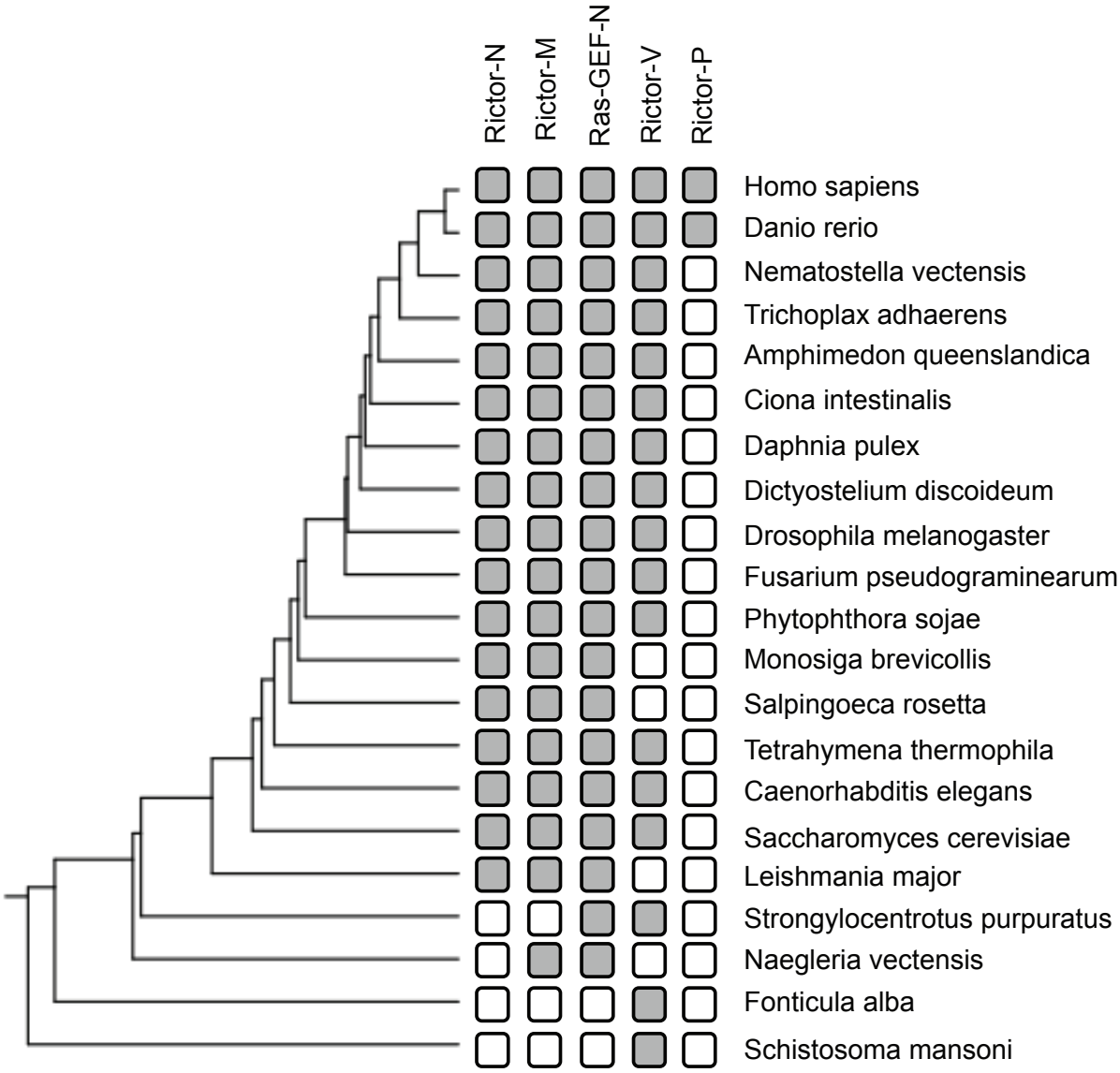

Occurrence chart of the Rictor conserved regions and the consensus cladogram.
Occurrence was determined by comparing the presence or the absence of the different Rictor conserved regions. The Rictor conserved regions were determined by domain searches using the Simple Modular Architecture Research Tool (smart.embl-heidelberg.de) program.
Filled squares indicate presence; open squares indicate absence.
Homo sapiens (Q6R327); *Danio rerio* (F1Q9T1); *Nematostella vectensis* (A7SRE9); *Trichoplax adhaerens* (B3S2G4); *Amphimedon queenslandica* (A0A1X7UI29); *Ciona intestinalis* (A0A3Q0K0X4); *Daphnia pulex* (E9HCD6); *Dictyostelium discoideum* (O77203); *Drosophila melanogaster* (X2JL73); *Fusarium pseudograminearum* (K3VWR9); *Phytophthora sojae* (G4YPP8); *Monosiga brevicollis* (A9V5T2); *Salpingoeca rosetta* (F2ULY1); *Tetrahymena thermophyla* (A4VDX0); *Caenorhabditis elegans* (G5EFN2); *Saccharomyces cerevisiae* (P40061); *Leishmania major* (Q4QB28); *Strongylocentrotus purpuratus* (W4Y7H9); Naegleria gruberi (D2UXA5); *Fonticula alba* (A0A058ZD18); *Schistosoma mansoni* (G4VPY8).

The consensus cladogram was constructed by using the CLUSTALW program (www.genome.jp/tools-bin/clustalW)

Fig. S2

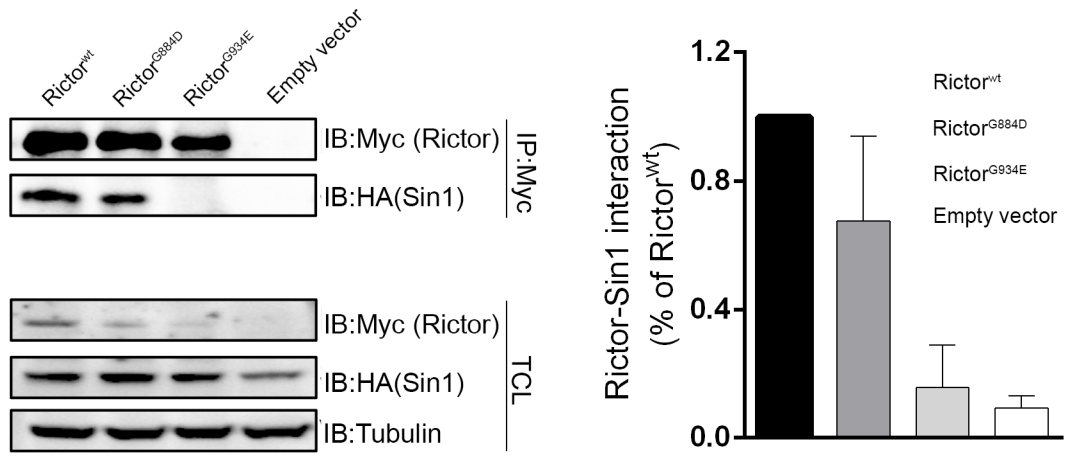

Rictor^{G884D} does not interfere with mTORC2 integrity.
Immunoprecipitation of Rictor in 293T co-transfected with Rictor mutants and Sin1. For immunoprecipitation myc-trap beads were used (all Rictor plasmids are myc-tagged). After one hour of incubation the immunocomplexes were carefully washed, subsequently clarified and analysed by Western blotting. Quantification of Sin-1 co-immunoprecipitated with Rictor was normalized on Sin1 values obtained with Rictor wild type form. Bar graph represents means of three independent experiments.

TABLE S1 Oligonucleotide sequences of the different primers

PRIMERS NAME	SEQUENCES
FORWRictorG934E H.s.	TGGGCCTTGGGAAATATCGAGTCATCAAATTGGGGTCTC
REVRictorG8934E H.s.	GAGACCCCAATTTGATGACTCGATATTTCCCAAGGCCCA
FORWRictorsG884D H.s.	GCCTATACACCTTTATGATCAACTAGTACACCATAAAACAGGC
REVRictorG884D H.s.	ATGGTGTACTAGTTGATCATAAAGGTGTATAGGCAGGTAGACG
FORWPia-Rictor^{G963E}	ATCGCAATTGGTCATATTGAGTCTTCTGTCGATGGTTATTC
REVPia-Rictor^{G963E}	GAATAACCATCGACAGAAGACTCAATATGACCAATTGCGAT